Zein-Based Ultrathin Fibers Containing Ceramic Nanofillers Obtained by Electrospinning. I. Morphology and Thermal Properties

Sergio Torres-Giner, Jose M. Lagaron

Novel Materials and Nanotechnology Group, IATA, CSIC, Apdo. Correos 73, Burjassot 46100, Spain

Received 8 October 2009; accepted 27 January 2010
DOI 10.1002/app.32180
Published online 26 May 2010 in Wiley InterScience (www.interscience.wiley.com).

ABSTRACT: This work presents the first results on the development and characterization of novel nanobiocomposite fibers prepared by electrospinning of zein/clay mixtures (from 99/1 to 75/25 wt/wt) from ethanol-based solutions. To do so, commercial ceramic materials of different nature, such as organomodified and unmodified mica, kaolinite, montmorillonite, and zeolite were employed and compared. A significant decrease in fiber diameter was observed as the clay fraction increased in the hybrid material. The highest clay contents also produced fibers but with extended beaded regions. All fillers nanodispersed well in the fibers at low loadings but unmodified mica particles were also seen excluded from the fibers, most likely due to excessive size. Surprisingly, the ceramic laminar structures, i.e. the phyllosilicates, were all seen to embed within the ultrathin fibers in what appears as an unreported rolled morphology due to the extensional forces generated by the electrospinning process. Electrospun nanobiocomposite fibers with optimal ceramic nanoparticle contents are currently investigated as an adequate procedure to prepare naturally occurring composite additives, coatings, and interlayers with enhanced performance in terms of mechanical, thermal, barrier, and control release properties for packaging, active packaging, biomedical, and pharmaceutical applications. © 2010 Wiley Periodicals, Inc. J Appl Polym Sci 118: 778–789, 2010

Key words: zein; nanocomposites; electrospinning; renewable polymers

INTRODUCTION

Electrospinning is a simple, versatile, and potentially low-cost method for making extremely ultrathin fiber-based structures from a wide range of natural polymers (biopolymers), from proteins to carbohydrates, and polymer blends.[1–3] This process entails placing a polymer solution into a syringe with a millimeter-size nozzle, which is subjected to high electric fields. Under these particular conditions, the polymer solution is ejected from the nozzle and deposited onto a collector, which also serves as ground. Furthermore, integration of the electrospinning process with conventional lithographic techniques will open up novel fabrication platforms for generating patterned microstructures from various materials and, over a broad range of length scales, for use in many application fields including active and bioactive packaging.[4,5]

Zein prolamine is the major storage protein of corn and comprises about 45–50% of its protein content. This protein has excellent outlook in the specialty food, pharmaceutical, and biodegradable plastics industry.[6] It has also been investigated for use as a fiber.[7] The material possesses the key properties of three other natural fibers, i.e. it has the comfort of cotton, the warmth of wool, and the hand of silk. Zein has also been reported to be easily spun by electrospinning from alcohol solutions to yield smooth fibers. The zein fiber diameter ranges from 50 nm to 6 microns and the mats consist of yarns of beads, tubular fibers, flat fibers, and ribbon-like fibers, depending on the conditions used for electrospinning as well as the zein solution properties.[1,8–11]

Natural occurring minerals, such as clays are usually hydrous aluminum phyllosilicates, sometimes with variable amounts of iron, magnesium, alkali metals, alkaline earths, and other cations which have structures of flat hexagonal sheets. Most clays are valuable minerals and can be then widely used in many industrial applications because of their high aspect ratio, plate morphology, natural abundance, and low cost. In this context, mica is a clay of the illite group which is composed of sheets of silicate tetrahedrons. The silicate sheets are composed of interconnected six membered rings, which are

Correspondence to: J. M. Lagaron (lagaron@iata.csic.es).
Contract grant sponsor: MEC; contract grant numbers: MAT2009-14533-C02-01, MAT2006-10261-C03.
Contract grant sponsor: EU FP6, NEWBONE.

responsible for mica's typical six sided pseudohexagonal symmetry. On the other hand, kaolinite clay is a naturally occurring 1 : 1 phyllosilicate containing a gibbsite (aluminum hydroxide) octahedral layer and a silicon oxide tetrahedral sheet. This asymmetric structure, which is typical of the group of the kaolin clays, allows the formation of hydrogen bonds between consecutive layers, providing a large cohesive energy. Montmorillonite (MMT), unlike kaolinite and other clays, displays a smectite-type structure, which strongly prone to swelling with increasing water content and is, therefore, a highly hygroscopic naturally occurring 2 : 1 phyllosilicate consisting of a central gibbsite octahedral layer between two external silica tetrahedral sheets. In its pristine form, MMT is readily miscible with hydrophilic polymers such as agropolymers. Zeolites, are microporous aluminosilicate minerals with well-defined structures, which are made up of four-connected networks of atoms, which generally results in a round structure. Because of their unique porous properties, zeolites result attractive for a wide range of applications.

As the above minerals, except zeolite, are expandable layered silicates, they can be intercalated and/or exfoliated into nanocomposites. Then, clay-containing polymeric nanocomposites comprise a polymeric matrix and dispersed in it mineral or synthetic clay platelets. For some polymers, the surface chemistry and polarity of the clays and minerals is not adequate to yield good interfacial adhesion and hence, incorporation of an organic modifier onto the clay surface, to mediate between the polarity of the hydrophilic clay surface and that of the more hydrophobic polymer, has been widely adopted for compatibilization and for ease of exfoliation of the clay platelets into the polymer matrix during processing. Depending on the functionality, packing density, and length of the organic modifiers, these materials can be engineered to optimize their compatibility with a given polymer. Surface modified clays have been studied as advanced additives to improve or balance thermal, mechanical, fire resistance, surface, or conductivity properties of many polymers because of its high surface-to-volume ratios and the subsequent intimate contact that they promote with the matrix at low filler additions.[12]

In contrast to conventional composites, where the reinforcement is on the order of microns, polymer nanocomposites can be exemplified by discrete constituents on the order of few nanometers. Specifically, by definition, a nanocomposite is a composite material in which at least one of the dimensions of the filler is in the nanometer range, this it to say, near or below 100 nm.[13] Through nanoscale engineering, it is then possible to combine the flexibility of natural proteins with the high strength and high modulus of inorganic nanoparticle components to produce a new array of agropolymer-based materials.[14] Several methods have been then considered to prepare biopolymer/layered silicates to generate a nanobiocomposite with an optimal dispersion of nanofillers. For instance, adding a small quantity of nanosized clay platelets can increase mechanical and physical properties of many biopolymers including higher gas barrier, greater stiffness, higher heat resistance, higher UV-resistance while maintaining transparency and impact property.[15–17] As a novel method, it is expected that the electrospinning of a polymer/clay combination can produce fiber mats with enhanced physical properties.[18]

Referring particularly to electrospun fibers, it has been first reported the generation of cylindrical and ribbon shaped fibers of nylon-6/MMT nanocomposites which ranged from 100 to 500 nm.[19] The process resulted in highly aligned MMT layers (layer normal perpendicular to the fiber axis) and nylon-6 crystallites (layer normal parallel to fiber axis). In other research,[20] multiwall carbon nanotubes were embedded in fibers of electrospun poly(ethylene oxide) as individual elements and most of which were aligned along the fiber axis. Electrospun polyurethane/organically modified MMT composites nanofibers, of diameter in the range of 150–410 nm, have also been reported.[21] The exfoliated MMT layers were well distributed within the polyurethane fibers and also oriented along the fiber axis. In another work, MMT nanosized platelets were incorporated into poly(L-lactic acid) solutions.[22] A nanobiocomposite fibrous structure which exhibited increased strength and improved structural integrity during biodegradation process was thus generated. Fibers of uniform diameters were obtained from poly(methyl methacrylate-*co*-methacrylic acid) containing MMT in recent research.[23] Dispersion of the clays within the fibers improved the electrospinnability of the resultant dispersions and MMT was predominantly exfoliated and well distributed within the fiber and oriented along the fiber axis. Char formation was observed when the clay-containing fibers were heated above the decomposition temperature, indicating a potential for reduced flammability and increased self-extinguishing properties. More recently, polystyrene/MMT clay fibers with diameters ranging from 4 μm to 150 nm were also prepared.[24] The addition of functionalized clays to the spinning solution produced fibers with a highly aligned MMT layer structure at a clay concentration of 4 wt %. The clay presence further enhanced the shear modulus of fibers and increased the glass transition temperature by nearly 20°C. Similar results have been also observed in nylon.[25] Furthermore, in the electrospinning of poly(ethylene oxide)/laponite fibers,[26] the enhanced physico-chemical properties of

the resultant fibers was related to the observed electrospun fiber morphologies.

The aim of this initial study is to prepare, for the first time, electrospun zein/clay nanobiocomposite ultrathin fiber mats to study the influence of the mineral nature on the morphology and thermal properties of the resultant fibers. The uses of such hybrid ultrathin structures will enable alternative approaches to fabricate coating, film, and fibers with enhanced mechanical, thermal, and control release properties.

EXPERIMENTAL

Materials

Zein from corn (grade Z3625) and ethanol of 96% v/v purity were purchased from Sigma-Aldrich (Spain) and Panreac (Spain), respectively. All products were used as received without further purification. Purified kaolinite, montmorillonite, zeolite, and mica minerals were supplied in powder form by Nanobiomatters S.L. (Spain). The company commercializes these minerals under the trademark of Nanobioter®. The organomodified mica, Nanobioter® AC11, contains about 30 wt % (as determined by TGA) of an organophilic modification. No further details of sample preparation or composition were disclosed by the manufacturer.

Electrospinning

Prior to the electrospinning process, composite solutions were fully dissolved, at room temperature, in ethanol/aqueous 85/15 (wt/wt) using various weight concentrations of zein/clay: 99 : 1, 95 : 5, 90 : 10, 85 : 15, 80 : 20, and 75 : 25 (wt/wt). An electrospinning assemble equipped with a variable high voltage 0–30 kV power supply was used. Further details of the basic setup can be found elsewhere.[1] All electrospinning experiments were carried out at 24°C in a controlled relative humidity chamber of 60%RH. The electrospinning process was done under the following conditions: 35 wt % zein/clay concentration, 0.30 mL/h flow-rate, 15 kV voltage, and 10 cm tip-to-collector distance. These optimum conditions were selected based on results from a previous study.[1] The minerals were dried under vacuum at 75°C for 48 h and then retained in desiccators set at 0%RH.

Viscosity

The viscosity of the polymer solutions was determined by a rotation viscometer VISCO BASIC PLUS L with a Low Viscosity Adapter (LCP), both from Fungilab S.A. (Spain).

Morphology

The morphology of the electrospun fibers was examined using scanning electron microscopy (SEM; Hitachi S-4100) after having been sputtered with a gold-palladium mixture in vacuum. All SEM experiments were carried out at 8.0 kV. Transmission Electron Microscopy (TEM) was performed using a JEOL 1010 (Japan) equipped with a digital BioScan image acquisition system from Gatan (USA). Zein fibers were directly electrospun on TEM grids and sizes measured by means of the Adobe Photoshop 7.0 software from the microscopic micrographs in their original magnification.

X-ray experiments

Wide angle X-ray experiments (WAXS) were performed using a Siemens D5000D equipment (Germany). Radial scans of intensity versus scattering angle (2Θ) were recorded at room temperature in the range 2 to 30° (2Θ) (step size of 0.03°(2Θ), scanning rate of 8 s/step) with identical settings of the instrument by using filtered Cu Kα radiation (k = 1.54 Å), an operating voltage of 40 kV, and a filament current of 30 mA. To calculate the clay basal spacing Bragg's law ($k = 2d \sin \Theta$) was applied.

Thermal analysis

Differential scanning calorimetry (DSC) analysis of typically 2 mg of the materials was conducted on a Perkin-Elmer DSC 7 (USA) thermal analysis system at a scanning speed of 10°C/min using N_2 as the purging gas. The thermal history applied was a first heating scan from 50 to 150°C to removed sorbed moisture, then cooling back to 50°C, and subsequent second heating scan from 50°C up to about 250°C. Before evaluation, the thermal runs were subtracted analogous runs of an empty pan. The DSC equipment was calibrated using indium as a standard. The T_g was estimated as the temperature of the maximum in the DSC thermograms. Thermal gravimetric analysis (TGA) was measured by a TG/ATD Setaram Setsys 16/18 (France), temperature was programmed from ambient to 800°C with a heating rate of 5°C/min in Argon. Sample mass was c.a. 10 mg.

RESULTS AND DISCUSSION

Morphology

Zein protein was readily soluble in ethanol 85 wt % and all clays were also dispersed in the polymer solution prior and during the electrospinning process up to clay contents of ca. 25 wt %. As can be seen from Table I, the solution viscosity decreased with increasing clay content. As lower solution viscosity

TABLE I
Viscosity of the Zein Solutions and Zein/Mineral Dispersions

Sample	Viscosity (cP)
Pure zein solution	137.39 ± 5.23
Zein/modified mica 99 : 1	133.04 ± 4.78
Zein/modified mica 95 : 5	127.93 ± 4.52
Zein/modified mica 90 : 10	119.25 ± 3.94
Zein/modified mica 85 : 15	104.84 ± 3.38
Zein/modified mica 80 : 20	89.46 ± 2.85
Zein/modified mica 75 : 25	75.42 ± 2.66
Zein/unmodified mica 99 : 1	132.18 ± 4.63
Zein/unmodified mica 90 : 10	115.27 ± 3.61
Zein/kaolinite 99 : 1	136.63 ± 5.18
Zein/kaolinite 90 : 10	116.85 ± 4.06
Zein/MMT 99 : 1	129.76 ± 4.69
Zein/MMT 90 : 10	112.46 ± 3.47
Zein/zeolite 99 : 1	135.41 ± 5.03
Zein/zeolite 90 : 10	121.98 ± 4.22
Zein 99 wt % of pure solution	132.12 ± 4.30
Zein 95 wt % of pure solution	123.45 ± 3.96
Zein 90 wt % of pure solution	111.95 ± 3.67
Zein 85 wt % of pure solution	92.08 ± 3.21
Zein 80 wt % of pure solution	76.96 ± 2.68
Zein 75 wt % of pure solution	62.79 ± 2.54

favors the formation of thinner fibers,[2] the average fiber size was seen to decrease with increasing clay contents due to the polymer concentration drop.

Typical SEM images of electrospun samples of zein/modified mica (wt/wt), as an example, are shown in Figure 1. It was observed that all nanobiocomposite fibers, independently of the clay nature, generated coarse tubular-like networks similar to those previously published for neat zein fibers.[1] The mayor morphological modification was produced at the highest clay content. In the latter samples, significant beaded structures appeared while the fibers became thinner.[27] Beaded morphologies were also observed when pure zein was electrospun at low concentrations (75 wt % of the original solution). Such structures have been recently encountered in the electrospinning of chitosan,[2] and in electrospun zein/chitosan blends.[3] Recent research has also suggested that polymer suspensions with good particle dispersion and high stability are capable of producing neat electrospun fibers without beading.[26]

The manifestation of other morphologies for electrospun zein (aside from beaded structures), such as flat ribbon-like and branched fibers, reported elsewhere,[28] were not observed. The appearance of beaded regions in the fibers may, on the other hand, be explained by the low viscosity values presented (Table I) as a result of the decrease in biopolymer concentration as the clay content increases in the suspension. The viscosity was even lower for suspensions of zein of same concentration but without minerals, hence supporting the viscosity argument in the observed morphology.

Figure 2 shows the changes in the diameter size distribution as a function of clay content. From this figure, it can be seen that the average fiber diameter decreased from ca. 390 to ca. 230 nm with increasing clay content and presented typical size distributions, with the exception of the highest content clay loading sample, in good agreement with previous research.[27] Nanocomposite fiber sizes ranged from ca. 80 up to ca. 700 nm.

Filler dispersion in the electrospun fibers

The distribution of the ceramic particles in the ultrathin fibers was investigated by bright field TEM imaging. In particular, from Figures 3 to 8 it is

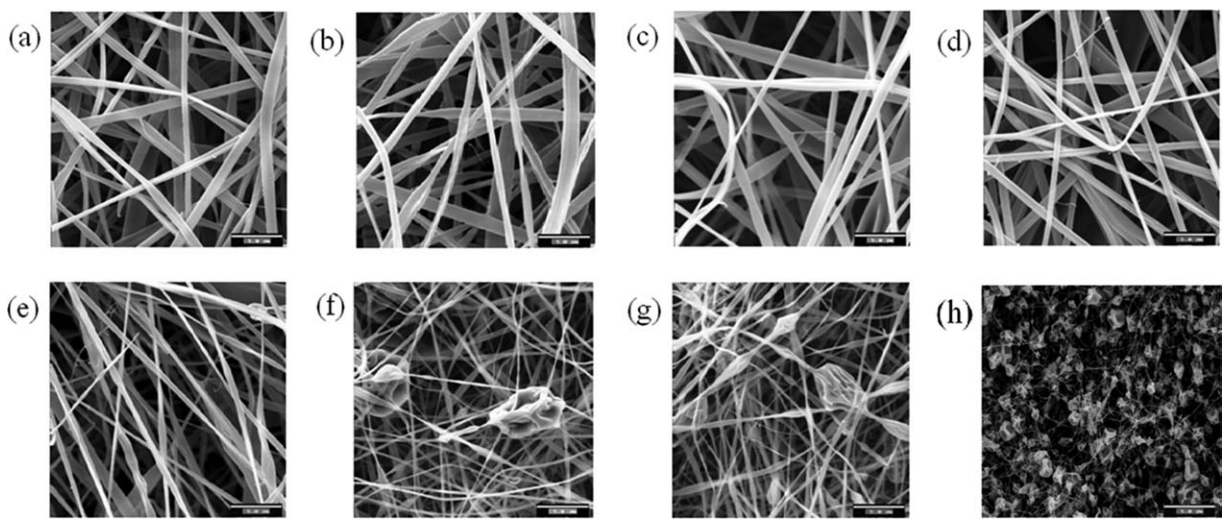

Figure 1 Typical SEM photographs of electrospun: (a) zein; (b) zein/modified mica 99 : 1 (wt/wt); (c) zein/modified mica 95 : 5 (wt/wt); (d) zein/modified mica 90 : 10 (wt/wt); (e) zein/modified mica 85 : 15 (wt/wt); (f) zein/modified mica 80 : 20 (wt/wt); (g) zein/modified mica 75 : 25 (wt/wt); (h) zein from 75 wt % of the pure zein solution. Scale markers of 5 μm in all cases.

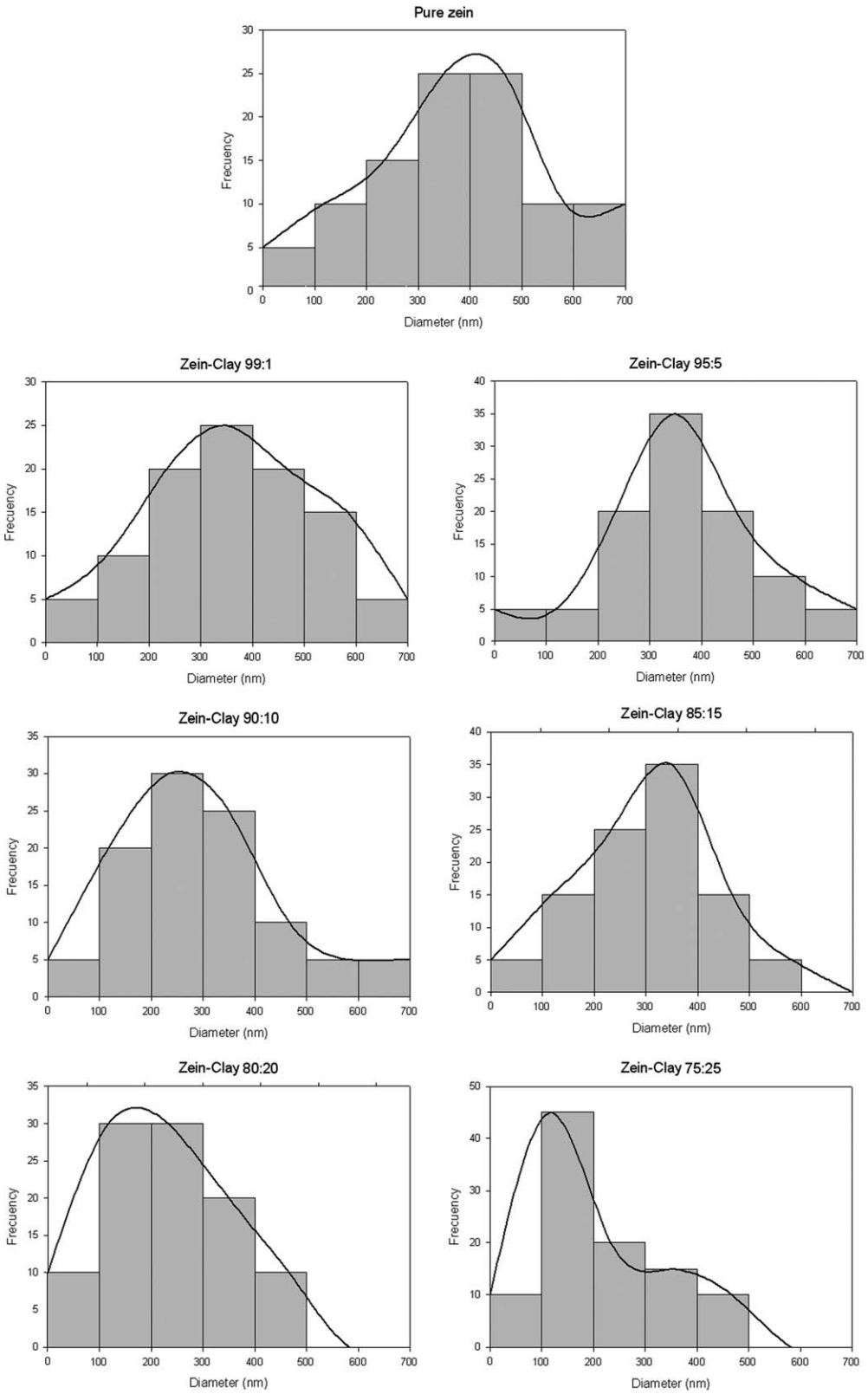

Figure 2 Influence of clay content (wt %) on fiber diameter size (nm) for electrospun zein/modified mica fibers.

shown typical and surprising TEM images of the electrospun nanobiocomposite fibers in which the dark zones are thought to represent the presence of the dispersed naturally occurring inorganic particles. From Figures 3 to 7, various morphologies can be observed inside the zein fibers, depending on the nature of the filler, all for the 95 : 5 (wt/wt) zein/ceramic compositions. Layers of unmodified mica clay

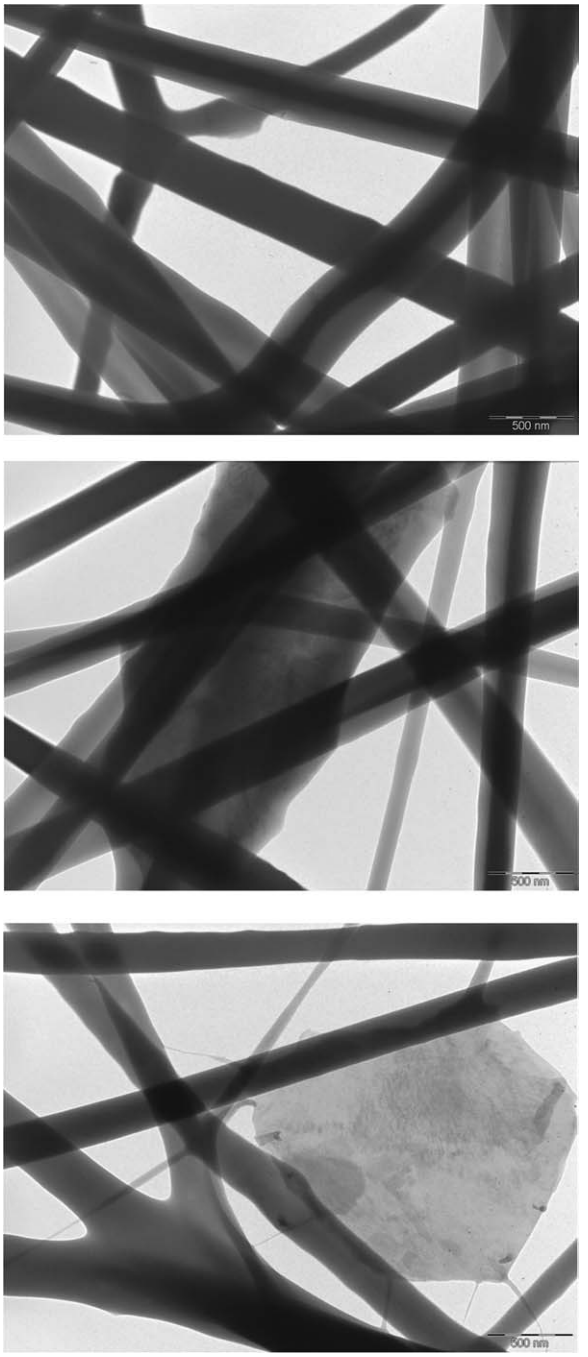

Figure 3 Selected TEM images of zein/mica 95 : 5 (wt/wt). Scale markers are 500 nm in all cases.

are seen inside the fibers but some bigger planar tactoids located outside the fibers (in orders of microns) can be seen in Figure 3. For the organomodified counterpart, Figure 4 shows that mica clay layers appear to be better distributed. Similar structures were observed for kaolinite in Figure 5. MMT clays were also well distributed along the zein fibers in Figure 6. On the other hand, in Figure 7, well dispersed zeolite spheres of diameters below 50 nm are seen as expected as natural zeolites are not laminar structures. Surprisingly and interestingly, most layered nanostructures, and this has not been, to the best of our knowledge, reported before, are seen embedded inside the fibers in what appears to be rolled morphologies oriented along the fiber axes direction. This may be a result of the extensional forces exerted by the electrospinning apparatus which could force the nanolayers to bend and align along the fiber axis, in agreement with previous research.[19,20,24,25] Unmodified mica, shows that some clay particles, maybe more aggregated structures, could not be bent by those forces and hence the particle is either trapped extended or excluded from the fiber (Fig. 3).

Although TEM images of fiber sections of 5 wt % mineral loaded samples confirmed that clay nanolayers seem to be well dispersed within the fibers, a very different observation occurs when the clay content increases. An apparent good dispersion was kept from 1 to 10 wt % of mineral content; however, for higher filler content fibers bigger agglomerates can be clearly seen in Figure 8. This could result, according to previous research,[24] from inhomogeneous distribution of ceramic particles

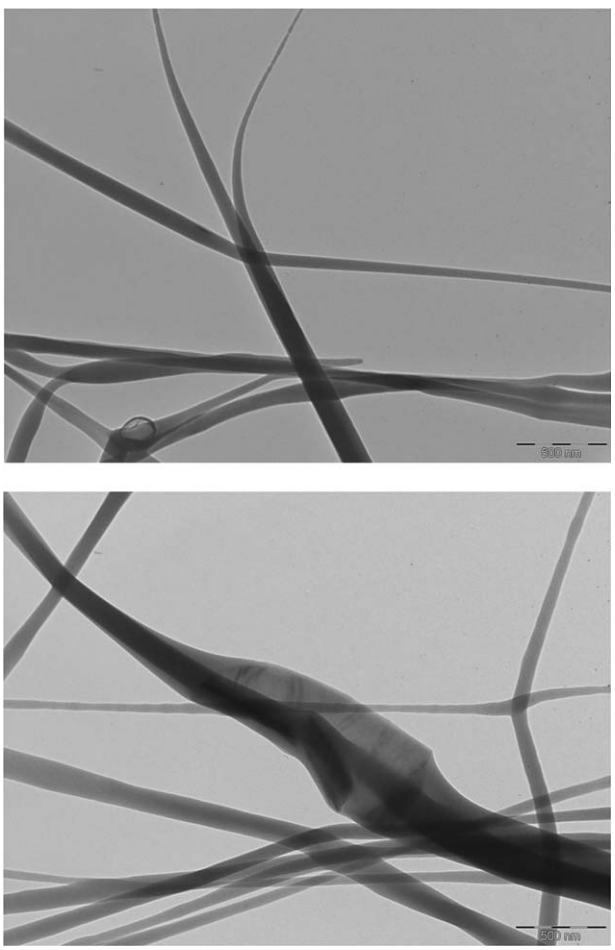

Figure 4 Selected TEM images of zein/modified mica 95 : 5 (wt/wt). Scale markers are 500 nm in all cases.

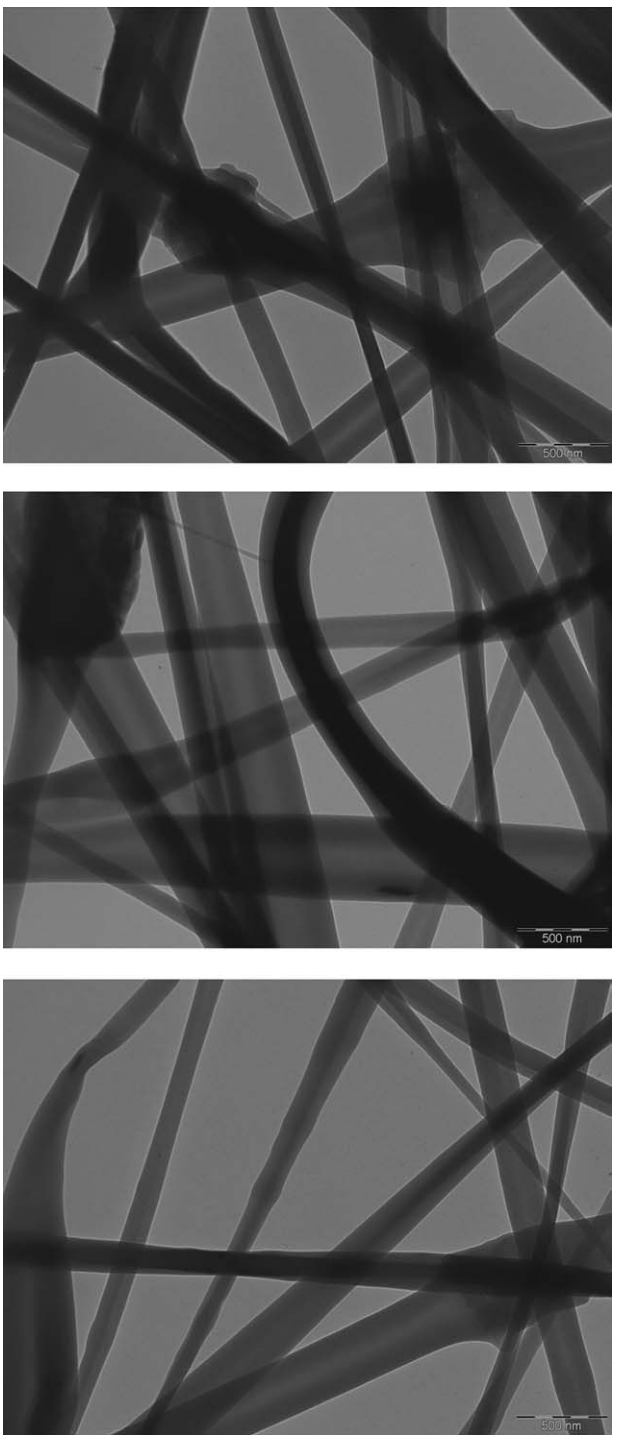

Figure 5 Selected TEM images of zein/kaolinite 95 : 5 (wt/wt). Scale markers are 500 nm in all cases.

due to solubility limits within the zein matrix. Dispersion is, in fact, not facilitated by fibers becoming thinner with increasing filler content due to the viscosity drop.

Finally, and in order to have alternative information about filler dispersion, the well reported WAXS patterns of the MMT clay system was measured (Fig. 9). From this Figure, it is seen that the basal peak of the unmodified MMT at 6.9°,[17] disappears in the composite fiber. The absence of this basal peak is related to separation of adjacent layers due to strong intercalation or exfoliation with the polymer matrix and hence supports the fact that a good clay dispersion within the zein fiber has been achieved at this loading.

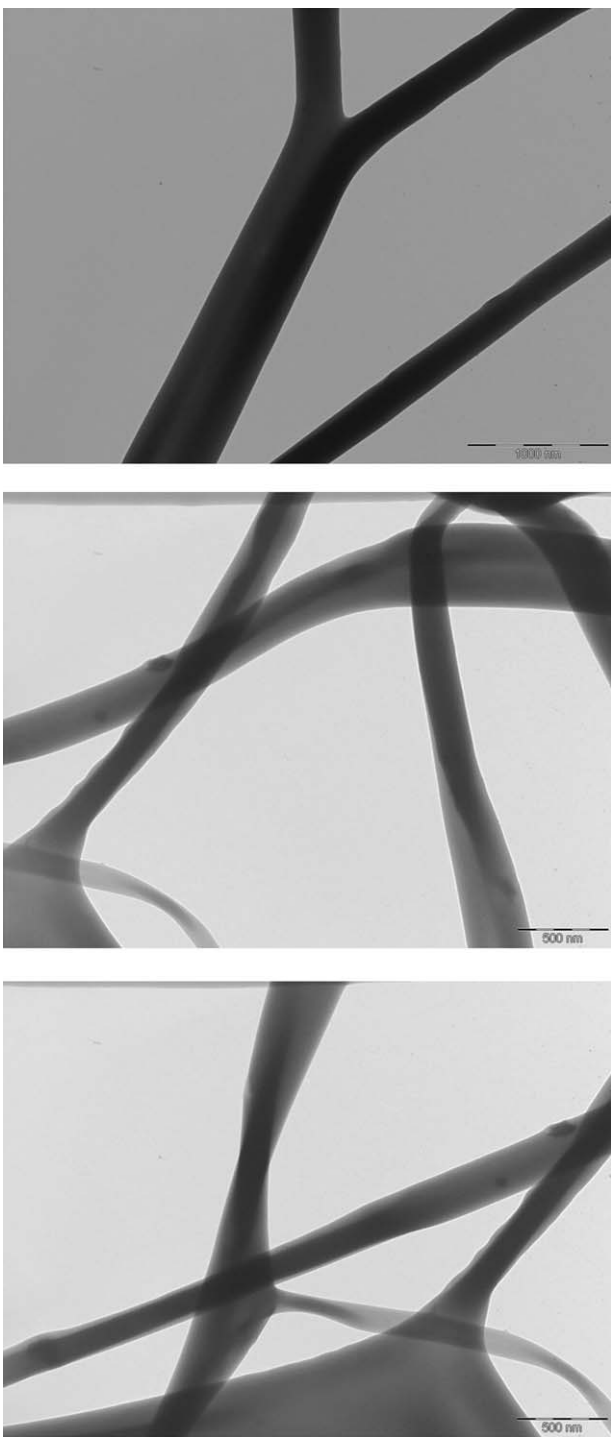

Figure 6 Selected TEM images of zein/MMT 95 : 5 (wt/wt). Scale markers are 500 nm in all cases.

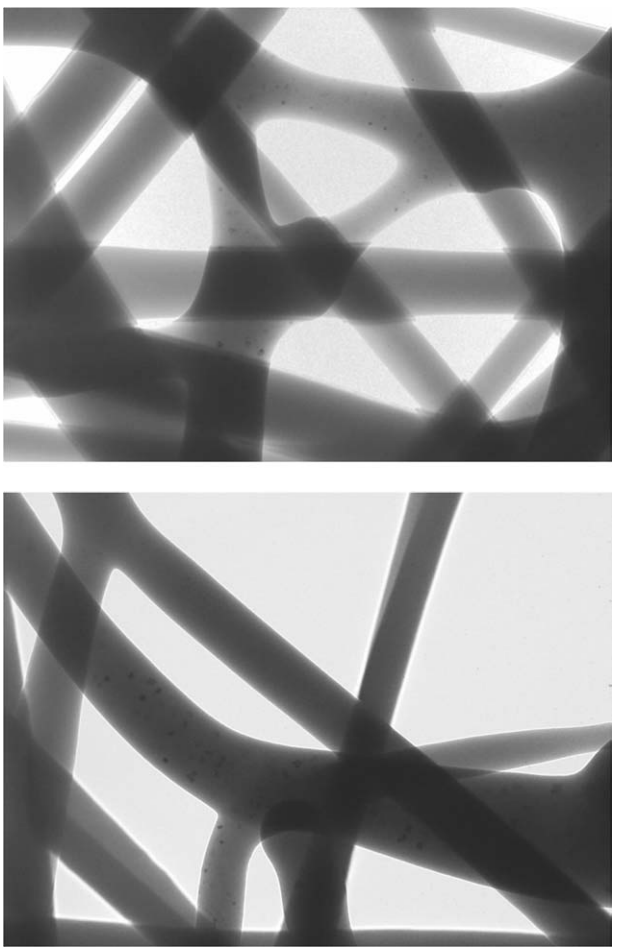

Figure 7 Selected TEM images of zein/zeolite 95 : 5 (wt/wt). Scale markers are 500 nm in all cases.

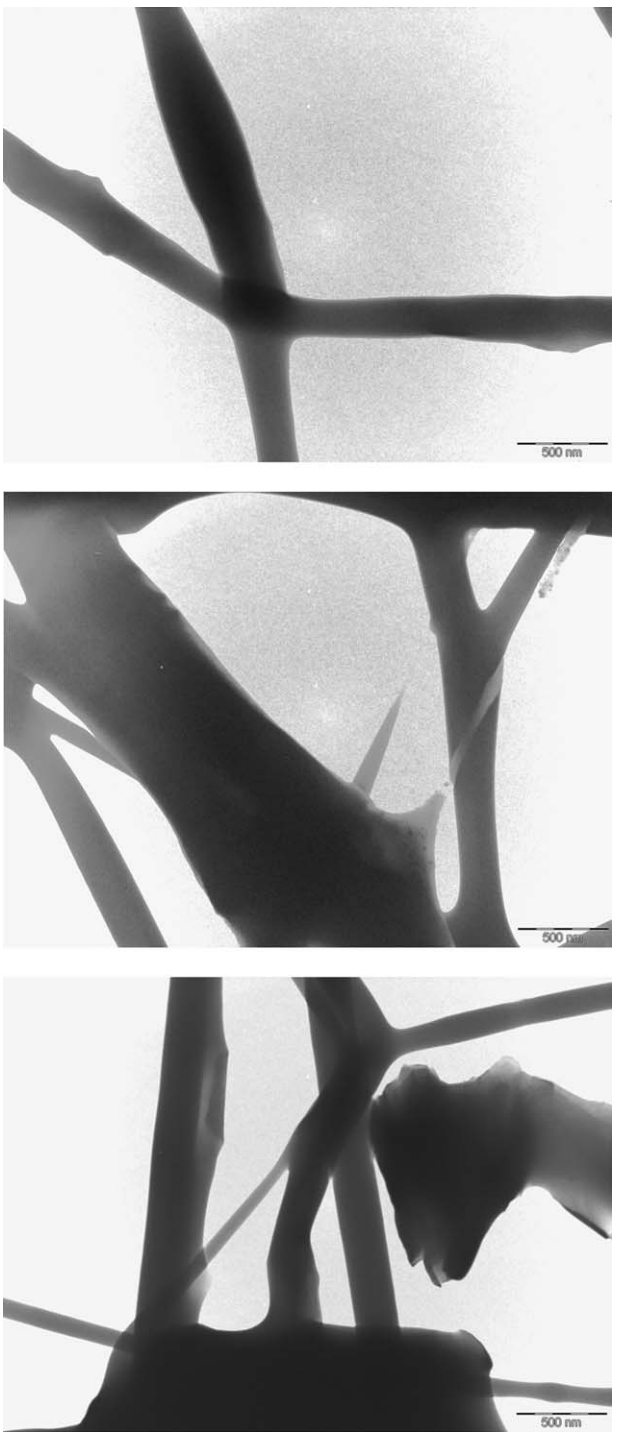

Figure 8 Selected TEM images of zein/modified mica, from top to bottom, of: 99 : 1 (wt/wt); 90 : 10 (wt/wt); 75 : 25 (wt/wt). Scale markers are 500 nm in all cases.

Thermal properties

The effect of the presence of the nanofiller on the thermal stability of the zein fibers was studied by means of DSC and TGA techniques, and the results are gathered in Table II. DSC was first used to evaluate the impact of ceramic particles on the zein glass transition temperature (T_g). Figure 10 plots, as an example, the typical DSC thermograms recorded in standard zein fibers (dotted line) and in zein/organomodified mica fibers (solid lines). This figure and the table show a T_g decrease in the electrospun fibers, especially at high ceramic concentrations. The decrease in the polymer T_g is, however, lower for kaolinite and unmodified mica and higher for the zeolite containing fibers. The reason for a T_g drop is usually plasticization of the polymer chains by the presence of flexibilizing agents or interchain self-associating disrupters. Ceramic particles are known to be more rigid than plastics and bioplastics but they are hydrophilic and carry and sorb moisture. To account for this fact, the materials were heat up to 150°C in an inert atmosphere within the DSC pan before the thermal scan from which the data was evaluated. This treatment should have been able to remove moisture from the samples and, therefore, the T_g drop must be attributed to intermolecular interception of zein by the dispersed ceramic particles. Thus, in this particular case, the ceramic particles may be regarded as reinforcing plasticizers.

TGA runs were finally carried out to determine the stability of zein fibers and of all other composites.

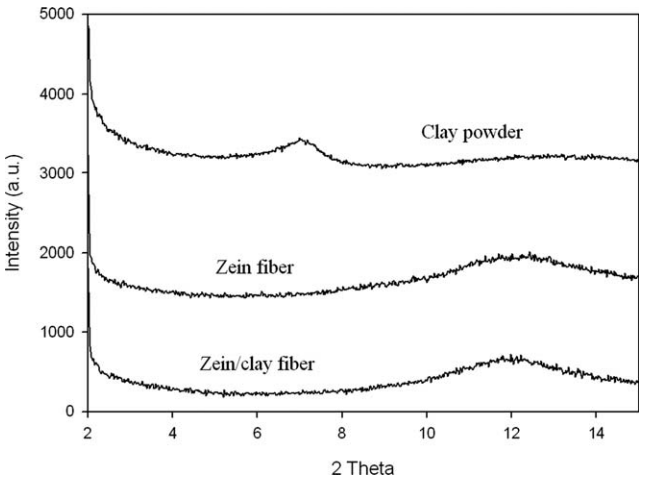

Figure 9 X-ray patterns of MMT clay powder, electrospun zein fiber, and the correspondent electrospun zein/MMT 95 : 5 (wt/wt).

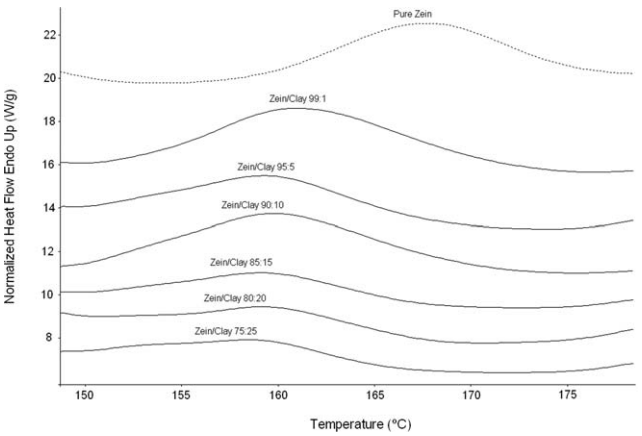

Figure 10 DSC thermograms in the glass transition region of the zein/modified mica fibers.

Figure 11 shows, as an example, TGA plots of standard zein fibers and zein/modified mica fibers. Three weight loss regimes can be observed in the TGA curves. A first weight loss occurs before 150°C, and is attributed to sorbed moisture and ethanol solvent from the samples (ca. 10 wt %). A second weight loss regime occurs between 150–450°C, and is related to thermal degradation of the zein biopolymer structure (ca. 50 wt %). Finally, a third weight loss regime appears at c.a. 600°C, associated to the carbonization of polymeric materials (ca. 40 wt %). According to previous research,[29] thermal degradation of zein prolamine usually starts at about 300°C. The first weight loss is then ascribed to degradation of the biopolymer network while the second loss corresponds to the degradation of the inner covalent bonds of the biopolymer monomers, in agreement with the thermal degradation characteristics of other polymers.[30,31] Ceramic materials are usually highly stable in air only suffering from dehydroxylation beyond 300ºC, nevertheless organoclays will begin to degrade the organic part even earlier but typically leaving residues of more than 75 wt % at 600ºC.[32]

For the second weight loss associated to pure zein fibers, it is observed in Figure 11 that the major weight loss occurred at ca. 295°C. This was consistent with the thermal patterns of electrospun zein reported recently.[1] When this value was compared to one of the organomodified mica-based composites, it was observed that the thermal stability of the fibers increased considerably with increasing the clay weight-percent. For the 99 : 1 (wt/wt) biopolymer/clay composition, the thermal resistance against degradation increased as the first derivative decreased to 311.51°C. This value was, in fact, the

TABLE II
T_g, Degradation Temperatures with Respective Weight Losses, and Residual Mass at 800°C for the Various Nanocomposite Fibers

	TGA data							
Sample	T_g (°C)	T_{d1} (°C)	Mass loss$_1$ (%)	T_{d2} (°C)	Mass loss$_2$ (%)	T_{d3} (°C)	Mass loss$_3$ (%)	Residual mass (%)
Pure zein	158.90	57.96	8.08	295.27	52.60	556.75	39.32	0.00
Zein/modified mica 99 : 1	156.91	56.54	3.27	311.51	51.35	589.58	44.82	0.56
Zein/modified mica 95 : 5	154.87	66.26	4.19	311.39	50.77	605.02	40.95	4.09
Zein/modified mica 90 : 10	152.75	77.78	5.22	308.84	49.03	609.26	37.39	8.36
Zein/modified mica 85 : 15	151.56	71.65	5.56	301.00	48.46	584.36	35.21	10.77
Zein/modified mica 80 : 20	150.26	78.71	6.53	282.83	47.04	575.30	33.01	13.42
Zein/modified mica 75 : 25	149.92	75.09	9.44	275.39	40.35	495.95	32.30	17.91
Zein/unmodified mica 99 : 1	158.14	56.38	2.73	307.57	50.78	580.29	45.58	0.91
Zein/unmodified mica 90 : 10	154.26	66.01	4.44	305.69	48.19	605.95	38.52	8.85
Zein/kaolinite 99 : 1	158.63	56.29	3.63	304.57	49.76	570.13	45,72	0.89
Zein/kaolinite 90 : 10	156.08	72.01	5.36	300.56	46.43	581.72	40.36	7.85
Zein/MMT 99 : 1	156.76	57.96	4.57	306.11	52.39	610.88	42.21	0.83
Zein/MMT 90 : 10	154.56	70.39	6.28	303.58	49.98	-	35.48	8.26
Zein/Zeolite 99 : 1	155.16	56.27	1.65	309.78	51.02	589.14	46.57	0.76
Zein/Zeolite 90 : 10	151.44	56.78	3.29	302.92	50.92	-	37.38	8.41

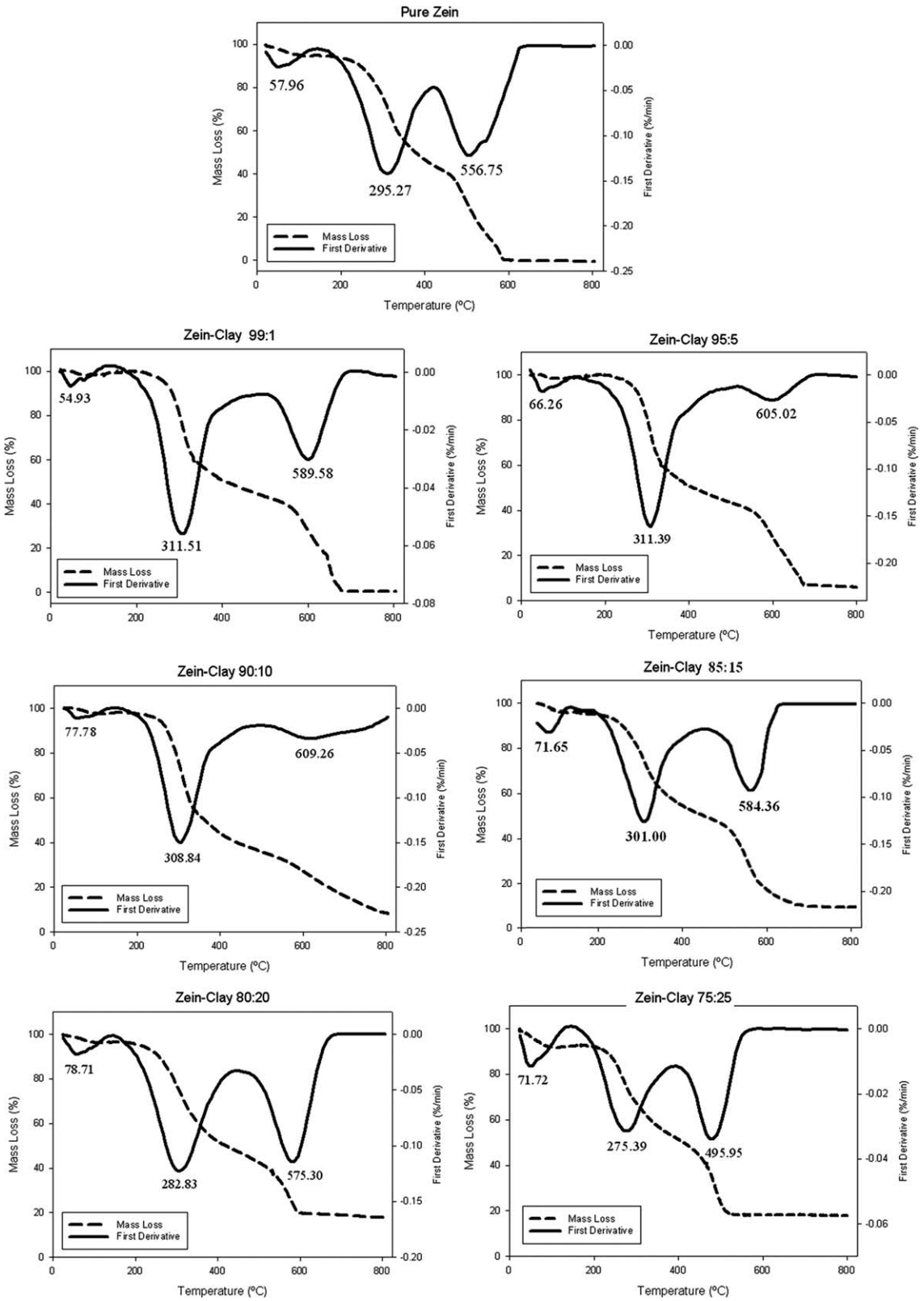

Figure 11 TGA mass loss and first derivative of zein/modified mica fibers.

largest observed for all clay contents which would indicate that the reinforcement effect on the nanobiocomposites fibers at this ratio was the largest. A similar thermal stability was held until ca. 10 wt % of clay content. The superior thermal performance can be attributed to the potential hindered diffusion of volatile decomposition products within the composites.[33] In spite of this, the thermal resistance of

composites between 15 and 25 wt % of clay were seen to decrease compared to lower loadings due to clay agglomeration acting as catalysts for degradation process and in excess of 20 wt % the stability was lower than that in the pure matrix.[34,35] In addition to this, it has also been reported that complex crystallographic structures and surface chemistry are inherent in clay minerals, which can result in catalytically active sites.[36] The latter effect would be more likely to occur in the event of poorly exfoliated clay layer structures or in excess of clay.

Third weight loss regimes observed in Figure 11 supported the above thermal results and showed that, for low ceramic particle contents, the nano-inorganic particles delayed the volatilization of the products originated by carbon–carbon bond scission in the biopolymer matrix. The major mass loss first derivative value increased from 556.7°C (pure zein) to 609.3°C (zein/clay 90 : 10). Interestingly, the third peak of the biopolymer associated to carbonization nearly vanished with increasing clay content up to 10 wt %. This effect is associated with a more gradual mass loss imposed by the impairing effect of higher loadings of the filler. This peak behaved similarly between materials but was least detectable for the case of MMT and zeolite. The degradation of inner covalent bonds of the zein matrix was sharper again at high clay contents, due to aggregation and high contents of ceramic particles. In general, the better results observed at low inorganic contents inside the zein fibers can be attributed to a good dispersion and orientation of the ceramic particles within the biopolymer during electrospinning by the high shear flow that applies in this process.[24]

CONCLUDING REMARKS

This first article reports about the morphology and thermal properties of novel nanobiocomposite ultrathin fibers obtained by electrospinning of zein and five commercial minerals with different contents. All the minerals were nanodispersed but curiously, the laminar phyllosilicates generally seemed to from rolled structures within the fibers most likely due to the extensional forces generated by the electrospinning process. Most minerals produced very similar physical values in terms of morphology and thermal stability. In all cases inorganic loading resulted to be the most impacting factor and all nanobiocomposites presented fiber thinning as well as beaded regions at high contents. Thermal stability of the zein matrix was improved below 10 wt % of mineral contents. The results were mainly explained by a collective effect of particle dispersion and orientation, which naturally occurred during the electrospinning process. A further study on the reinforcing properties, in terms of mechanical and barrier, of these particular additives is currently being carried out within biopolymer matrices.

The electrospun fibers developed could be applied as reinforcing naturally occurring hybrid nanostructures of potential interest in coatings, packaging, and other applications. Of particular interest is the design of functional packaging nanoaditives, coatings, or interlayers for food and beverages, in which the nanobiocomposite fibers can reinforce mechanical, thermal, and barrier properties of both plastic and bioplastic matrices without losses in biodegradability and optical properties. In active food packaging, pharmaceutical and biomedical applications they could also be used for the control release of actives or bioactives.

Nanobiomatters S.L. is also acknowledged for supplying materials.

References

1. Torres-Giner, S.; Gimenez, E.; Lagaron, J. M. Food Hydrocolloids 2008, 22, 601.
2. Torres-Giner, S.; Ocio, M. J.; Lagaron, J. M. Eng Life Sci 2008, 8, 303.
3. Torres-Giner, S.; Ocio, M. J.; Lagaron, J. M. Carbohydr Polym 2009, 77, 261.
4. Lagaron, J. M.; Gimenez, E.; Sanchez-Garcia, M. D.; Ocio, M. J.; Fendler, A. Presented at the 15th IAPRI World Conference in Packaging; Tokyo, Japan, 2006.
5. Busolo, M. A.; Torres-Giner, S.; Lagaron, J. M. Enhancing the Gas Barrier Properties of Polylactic Acid by Means of Electrospun Ultrathin Zein Fibers. Annual Technical Conference – ANTEC, Conference Proceedings 2009, 5, pp. 2763–2767.
6. Corradini, E. A.; Souto de Medeiros, E.; Carvalho, A. J. F.; Curvelo, A. A. S.; Mattoso, L. H. C. J Appl Polym Sci 2006, 101, 4133.
7. Shukla, R.; Cheryan, M. Ind Crops Prod 2001, 13, 171.
8. Miyoshi, T.; Toyohara, K.; Minematsu, H. Polym Int 2005, 54, 1187.
9. Chen, Y.; Xinsong, L.; Tangying, S. J Appl Polym Sci 2007, 103, 380.
10. Jiang, H.; Zhao, P.; Zhu, K. Macromol Biosci 2007, 7, 517.
11. Selling, G. W.; Biswas, A.; Patel, A.; Walls, D. J.; Dunlap, C.; Wei, Y. Macromol Chem Phys 2007, 208, 1002.
12. Hwu, J. M.; Jiang, G. J.; Gao, Z. M.; Xie, W.; Pan, W. P. J Appl Polym Sci 2002, 83, 1702.
13. Lagaron, J. M.; Cabedo, L.; Cava, D.; Feijoo, J. L.; Gavara, R.; Gimenez, E. Food Adit Contam 2005, 22, 994.
14. Angellier-Coussy, H.; Torres-Giner, S.; Morel, M.-H.; Gontard, N.; Gastaldi, E. J Appl Polym Sc 2008, 107, 487.
15. Sanchez-Garcia, M. D.; Gimenez, E.; Lagaron, J. M. J Plast Film Sheet 2007, 23, 133.
16. Sanchez-Garcia, M. D.; Gimenez, E.; Ocio, J. M.; Lagaron, J. M. J Plast Film Sheet 2008, 24, 239.
17. Sanchez-Garcia, M. D.; Gimenez, E.; Lagaron, J. M. J Appl Polym Sci 2008, 108, 2787.
18. Vaia, R. A.; Wagner, H. D. Mater Today 2004, 7, 32.
19. Fong, H.; Liu, W. D.; Wang, C. S.; Vaia, R. A. Polymer 2002, 43, 775.
20. Dror, Y.; Salalha, W.; Khalfin, R. L.; Cohen, Y.; Yarin, A. L.; Zussman, E. Langmuir 2003, 19, 7012.

21. Hong, J. H.; Jeong, E. H.; Lee, H. S.; Baik, D. H.; Seo, S. W.; Youk, J. H. J Polym Sci Part B: Polym Phys 2005, 43, 3171.
22. Lee, Y. H.; Lee, J. H.; An, I.-G.; Kim, C.; Lee, D. S.; Lee, Y. K.; Nam, J.-D. Biomaterials 2005, 26, 3165.
23. Wang, M.; Hsieh, A. J.; Rutledge, G. C. Polymer 2005, 46, 3407.
24. Ji, Y.; Li, B.; Ge, S.; Sokolov, J. C.; Rafailovich, M. H. Langmuir 2006, 22, 1321.
25. Li, L.; Bellan, L. M.; Craighead, H. G.; Frey, M. W. Polymer 2006, 47, 6208.
26. Daga, V. K.; Helgeson, M. E.; Wagner, N. J. J Polym Sci Part B: Polym Phys 2006, 44, 1608.
27. Saeeda, K.; Parka, S.-Y.; Leeb, H.-J.; Baekb, J.-B.; Huh, W.-S. Polymer 2006, 47, 8019.
28. Koombhongse, S.; Liu, W. X.; Reneker, D. H. J. J Polym Sci Part B: Polym Phys 2001, 39, 2598.
29. Magoshi, J.; Nakamura, S.; Murakami, K. I. J Appl Polym Sci 1992, 45, 2043.
30. Li, X.-G. React Funct Polym 1999, 42, 53.
31. Winslow, F. H.; Matreyek, W. J Polym Sci 1956, 22, 315.
32. Bertini, F.; Canetti, M.; Audisio, G.; Costa, G.; Falqui, L. Polym Degrad Stab 2006, 91, 600.
33. Gilman, J. W.; Jackson, C. L.; Morgan, A. B.; Harris, R.; Manias, E.; Giannelis, E. P.; Wuthenow, M.; Hilton, D.; Phillips, S. H. Chem Mater 2000, 12, 1866.
34. Tang, Y.; Hu, Y.; Song, L.; Zong, R.; Gui, Z.; Chen, Z.; Fan, W. Polym Degrad Stab 2003, 82, 127.
35. Qin, H.; Zhang, S.; Zhao, C.; Feng, M.; Yang, M.; Shu, Z.; Yang, S. Polym Degrad Stab 2004, 85, 807.
36. Davis, R. D.; Gilman, J. W.; Vanderhart, D. L. Polym Degrad Stab 2003, 79, 111.